Upgrading of methane emissions via chemical looping over copper-zeolites: Experiments and modelling

Mauro Álvarez, Pablo Marín, Salvador Ordóñez *

Catalysis, Reactors and Control Research Group (CRC), Dep. of Chemical and Environ. Engineering, University of Oviedo, Julián Clavería 8, 33006 Oviedo, Spain

HIGHLIGHTS

- Methanol obtained from methane by a looping process based on Cu-mordenite.
- At anaerobic conditions, high CH_4 pressures increase CH_3OH selectivity.
- Equilibrium and kinetic models were proposed for methane chemisorption.
- Methanol productivity decreased at aerobic conditions due to over-oxidation.

GRAPHICAL ABSTRACT
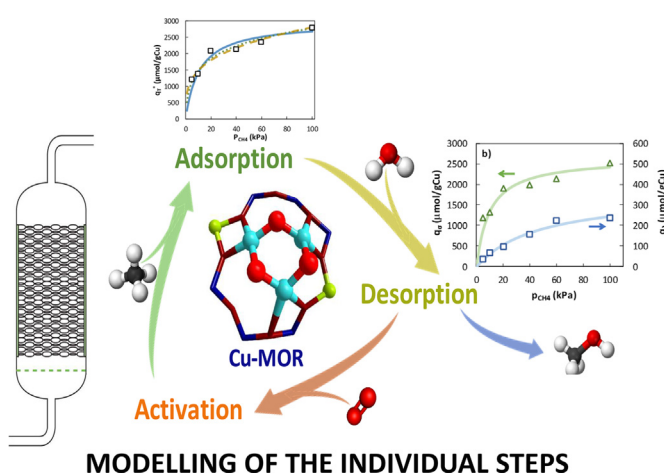
MODELLING OF THE INDIVIDUAL STEPS

ARTICLE INFO

ABSTRACT

The interest in methane direct conversion into methanol has increased in the last years. A copper-mordenite looping process, based on the separation of methanol formation (200 °C) and copper re-activation (450 °C), has been studied. Methane partial pressure (studied in the range 5–100 kPa) had a positive effect on methanol productivity (10.7 μmol/g zeolite at 100 kPa CH_4). It was found that the adsorption time had some impact on the productivity; a minimum value of 60 min was needed to reach the equilibrium. Using the experimental results, the equilibrium and kinetics of methane chemisorption were modelled. The proposed model is based on the formation of two adsorbed species: methoxy and CO_2-precursors.

Many methane emissions and feedstocks are diluted and contain oxygen. Thus, methane adsorption has also been studied at aerobic conditions, to apply the looping conversion of methane into methanol to these sources. High oxygen concentrations were considered (2.5–16 mol%), resulting in a decrease in methanol productivity and the over-oxidation of most adsorbed CO_2-precursors during the adsorption step. The model was updated for considering the over-oxidation to CO_2.

© 2022 The Author(s). Published by Elsevier Ltd. This is an open access article under the CC BY-NC-ND license (http://creativecommons.org/licenses/by-nc-nd/4.0/).

1. Introduction

Nowadays, a sharp decrease in the emissions of global warming gases has become the main technological challenge. Among these

* Corresponding author.
  E-mail address: sordonez@uniovi.es (S. Ordóñez).

gases, methane has a key role, because of having a global warming potential 28 times higher than that of CO_2 (Jackson et al., 2019; Pratt and Tate, 2018). Many methane emissions cannot be avoided, such as, those of waste and wastewater treatment plants, abandoned coal mines, etc. (Karakurt et al., 2012; Saunois et al., 2016). When methane is extracted as side product in oil fields, it is usually flared on the spot, especially on remote locations, because transportation costs are too high (Tomkins et al., 2017; Kulkarni et al., 2018). The combustion to CO_2 reduces the environmental impact of these emissions, but its energetic potential is wasted. This fact results in a yearly loss of ca. 140 billion cubic meters of methane (Latimer et al., 2018). Furthermore, emissions with high volumetric flow rates, low methane concentration and contamination with oxygen from air (very common in sectors as agriculture, water management and coal mining), are not appropriate for direct flaring (Su et al., 2005; Hoglund-Isaksson et al., 2012).

Some authors have proposed the catalytic combustion of methane as the best option to reduce the global warming potential of methane and, simultaneously, exploit the energy of these low concentration emissions (Fernández et al., 2016; Marín et al., 2019; Marín et al., 2020). However, due to the constant increase of worldwide energy demand, the transformation of these diluted methane emissions into a liquid fuel, such as, methanol is a more interesting alternative (Hammond et al., 2012; Sun et al., 2020). The transportation, storage and handling costs of methanol are much lower than that of methane and its energy density is higher (Hammond et al., 2012; Zakaria and Kamarudin, 2016). Methanol is one of the most attractive and versatile molecules in the chemical industry and its production is expected to keep increasing. Apart from its use as gasoline additive, methanol is used in many processes as raw material and solvent (Khirsariya and Mewada, 2013).

The commercial process of methane conversion into methanol is based on the formation of a synthesis gas via steam reforming, followed by catalytic conversion into methanol. This process is not suitable for many methane sources and emissions, like diluted emissions containing oxygen (Han et al., 2016; Olivos-Suarez et al., 2016; Chaemwinyoo et al., 2022). Thereupon, a technology capable of converting methane into methanol in only one step and at softer conditions is highly desirable to exploit methane emissions with untapped potential (Palkovits et al., 2010; Mahyuddin et al., 2019).

The main problem of this process is the stability of the C-H bond of methane. Its high bond energy (415 kJ/mol) makes it necessary the search for a strategy to avoid the overoxidation of partially oxidized products to CO_2 (Liu and Du, 2018; Jocz et al., 2019). It is known that in nature methanotrophic bacteria can oxidize methane to methanol with high selectivity at room temperature by the iron and copper on their soluble and particulate methane monoxygenase enzymes (Al-Shihri et al., 2020). The use of zeolites is one of the most interesting options for replicating this natural process. Zeolites are stable well-known materials that can stabilize oxygen-bridging centres of some metals and mimic the active centres of methanotrophic bacteria enzymes (Burnett et al., 2019). Previous promising results have been obtained using copper-exchanged mordenites (MOR). The structure of MOR zeolites is made of main 12MR pores (7.0x6.5 Å) connected by narrower 8MR channels (5.7x2.6 Å). The smaller 8MR channels provide a perfect framework for the exchange of copper and formation of active centres, while the larger 12MR channels facilitate reactant and product transport (Grundner et al., 2015; Pappas et al., 2018; Mahyuddin et al., 2018). Copper-ion-exchanged mordenite has been known to have various copper active sites, which feature monomeric, dimeric, and trimeric copper species (Jeong et al., 2021). The μ-oxo dicopper active sites, $[Cu_2(\mu\text{-O})]^{2+}$, have been widely reported as an active species in the conversion of methane to methanol (Knorpp et al., 2018). These copper oxides hosted on

the zeolite structure can cleave the C-H bound of methane with activation energies of 60 kJ/mol (Mahyuddin et al., 2018).

The copper-zeolite active sites are highly hydrophilic and not stable in trace amounts of water. For this reason, they require high activation temperatures (>350 °C, typically 450 °C) in the presence of oxygen (or air) and the complete removal of water from the zeolite structure (Knorpp et al., 2018). Then, the reaction with methane is conducted at 200 °C (a lower temperature would decrease the amount of activated methane) (Zheng et al., 2020). The interaction of methane with the active centres generates methoxy intermediates, which are strongly linked to the active centres and require protic solvents for the removal of the methanol product (Sheppard et al., 2016). Hence, a third step where a water stream is introduced at 150 °C is required (Sushkevich et al., 2020; Sheppard et al., 2014). In order to reactivate the active centres and remove all the water from the zeolite structure, a new activation step is needed (Sheppard et al., 2014; Knorpp et al., 2018). In this kind of stepwise operation, for each active centre a maximum of one methane molecule can be converted per reaction cycle. This means that the active sites are operating stoichiometrically instead of catalytically. However, it is also known that copper-zeolites can also operate catalytically at steady state in the simultaneous presence of water and methane but requiring higher temperatures to promote methane conversion (Sun et al., 2021).

In previous works, the activation and desorption steps were optimized to maximize methanol yield (Álvarez et al., 2020; Álvarez et al., 2021). It was also observed that only some active sites can transform methane into methanol. The aim of the present work is to perform a modelling analysis of the looping process at anaerobic and aerobic conditions. The presence of oxygen and low methane concentration opens the door to valorisation of non-exploited methane sources and emissions. To the best of our knowledge, this is the first study dealing with this issue, despite the practical interest for the harnessing of these methane sources.

2. Materials and methods

2.1. Catalyst preparation

The support used to prepare the catalyst is a commercial Na-Mordenite (Na-MOR) zeolite with a Si/Al ratio of 13 from Zeolyst International. The technique used for its preparation is aqueous ion exchange with a 0.01 M copper (II) acetate solution (Grundner et al., 2015; Grundner et al., 2016). The pH is kept at 5.7 to avoid the precipitation of copper hydroxides, maximizing the copper content on the zeolite. One gram of zeolite is added per 78 ml of solution and the mixture is stirred overnight at room temperature. Then, the solid is filtered, washed and mixed with a new fresh copper acetate solution; this procedure is repeated three times. After the last ion exchange the solid is dried at 110°C, pelletized and sieved to a particle size between 0.355 and 1 mm. In order to activate the catalyst, it is loaded into a stainless steel reactor and heated up to 450°C (1°C/min rate) in air flow (Alayon et al., 2012). This procedure leads to a copper loading of 4.5 wt%, measured by ICP–MS, which is consistent for different batches of catalyst. The characterization of the catalyst was performed and explained in previous publications (Álvarez et al., 2020).

2.2. Experimental device and procedure

2.2.1. Experimental device

The experiments were performed in a 600 mm length stainless steel fixed-bed reactor (ID = 6.8 mm). The copper-mordenite (3 g, particle size of 0.335–1 mm) was placed inside the reactor (110 mm bed length), which was heated by an electrical oven.

Temperature was measured inside the reactor (closed to the solid bed). The gases were supplied as cylinders (Air Liquide) and the requested flowrate and concentration were obtained using mass flow controllers (Bronkhost). The liquid (water) was introduced using a syringe pump. Heating tape was used to maintain pipes at 150°C and prevent condensations. The reactor effluent was sent to a cold trap, where condensable species were recovered. Pressure was maintained at 100 kPa for all the tests. Two analytical techniques were used: an on-line quadrupole mass spectrometer (MS, Pfeiffer Omnistar) and a gas chromatograph (GC, Shimadzu GC-2010 equipped with CP-Sil 8CB column and FID).

2.2.2. Experimental procedure

The looping process for copper-doped zeolites consists of three cyclic steps: solid activation, methane chemisorption and methanol desorption. The following methodology has been optimised in previous publications (Álvarez et al., 2020; Álvarez et al., 2021).

First, the copper-mordenite was activated at high temperature (450°C) in a stream of air for 4 h. The use of air, instead of pure oxygen, was found to be beneficial for the production of methanol, as explained elsewhere (Álvarez et al., 2021).

Then, the methane chemisorption step was performed at 200°C, the optimum temperature for this chemical looping process (Zheng et al., 2020), using a total gas flow rate of 0.12 NL/min and different methane concentrations. In this context, two scenarios were considered: methane diluted in nitrogen (5–100 mol% methane) and methane diluted in poor air (0–16 mol% oxygen). It should be noted that most literature studies performed the adsorption with pure methane or methane-inert mixtures. In the scope of a previous work (Álvarez et al., 2021), it was demonstrated that this step can also be accomplished in the presence of oxygen, which is more practical for the upgrading of methane emissions.

During the chemisorption step, the on-line MS was used to monitor the different compounds involved in the reaction: methane, methanol and CO_2. The total amount of chemisorbed methane was quantified by temperature programmed oxidation (TPO) tests, done after the adsorption step. Since methane is strongly linked to the active sites, isothermal desorption cannot be used to quantify the zeolite capacity. The increase of temperature (10 °C/min ramp until 450 °C) during the TPO test favours the complete oxidation of methane to CO_2, which was measured on-line by the mass spectrometer (the signal attributed to CO_2 was calibrated using bicarbonate standards). The accuracy of this analysis was checked by repeating the procedure at the same conditions to calculate the confidence interval and relative error: for a chemisorption with 100 mol% methane, the total CO_2 released in the TPO was 2798 ± 76 µmol g Cu^{-1} (relative error of 3%).

Finally, the methanol desorption step was carried out just after the adsorption one. The release of methanol to the gas phase was forced using a water/nitrogen gas stream (0.16 NL/min, 5.2 mol% water). Desorbed methanol and water were condensed in the cold trap and collected; these liquid samples were quantified by GC–FID. The accuracy of this sample and analytical procedure was also checked. Thus, for a chemisorption with 100 mol% methane, methanol productivity was 237 ± 9 µmol g Cu^{-1} (relative error of 4%).

3. Results and discussion

3.1. Reaction scheme at anaerobic conditions

The looping methane partial oxidation consists of three cyclic steps: solid activation, methane chemisorption and methanol desorption. Fig. 1 shown the results of the reaction for experiments at anaerobic conditions with different methane partial pressure.
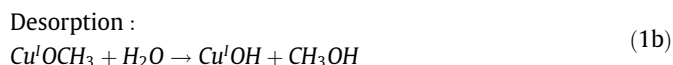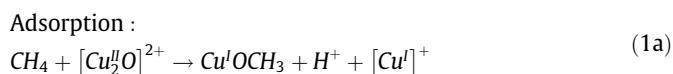
Methanol productivity (q_{CH_3OH}) was determined by the analysis of methanol in the liquid samples collected from the cold trap during the desorption step. In all the reaction experiments, even in those with the highest productions, no by-products were detected in the liquid samples; methanol was the only product detected and quantified by GC–MS and GC–FID.

During methane chemisorption, the reactor effluent was monitored using the on-line MS. No methanol or CO_2 was detected at anaerobic conditions. The productivity of CO_2 (q_{CO_2}) was calculated as the difference between the total amount of chemisorbed methane (measured by a TPO carried out after the chemisorption step, as explained in section 2.2.2) and methanol productivity (measured in the liquid sample taken during the desorption step). Hence, the CO_2 productivity accounts for the methane molecules that, at the end of the chemisorption step, are adsorbed as CO_2 precursors, like surface formiate intermediates.

The experiments show that methane partial pressure has a positive influence on both methanol and CO_2 productivities (Fig. 1a). Selectivity to methanol (ratio of methanol productivity to the total methane adsorption) also increases as methane partial pressure increases (Fig. 1b). Thus, methanol selectivity can be raised up to 9% for 100 kPa CH_4.

The temperature-programmed-oxidation tests, carried out after methane chemisorption, revealed the presence of two CO_2 peaks at different temperatures (Álvarez et al., 2021). This finding is attributed to active sites of different strength or with different chemisorbed species (e.g., methoxy or CO_2 precursors).

Copper dimeric species has been identified as responsible of methane activation. They can be stabilized in a mordenite pore and provide two electrons to convert methane to methanol (Jeong et al., 2021). The formation of methanol by a single mono-µ-oxo dicopper (II) site, $[Cu_2O]^{2+}$, has been described extensively in the bibliography. Spectroscopic studies have provided evidence that methanol formation over Cu zeolites involves the formation of methoxy (or adsorbed methanol) surface intermediates (reaction (1a)) (Brezicki et al., 2021). These methoxy species formed during the adsorption step are removed from the zeolite in the desorption step with the help of water (reaction (1b)).

Adsorption :
$$CH_4 + \left[Cu_2^{II}O\right]^{2+} \rightarrow Cu^IOCH_3 + H^+ + \left[Cu^I\right]^+ \tag{1a}$$

Desorption :
$$Cu^IOCH_3 + H_2O \rightarrow Cu^IOH + CH_3OH \tag{1b}$$

The formation of CO_2 may proceed via the formation of surface formiate intermediates over the copper zeolites. These intermediates have been detected using spectroscopic techniques during the methane activation reaction and have been claimed to be precursors to CO_2 (Sushkevich and van Bokhoven, 2018; Sushkevich et al., 2020). Recently, it has been suggested that µ-1,2-peroxo dicopper (II) species are responsible of CO_2 formation (Brezicki et al., 2021):

$$CH_4 + 2\left[Cu_2^{II}O_2\right]^{2+} \rightarrow CO_2 + 2H_2O + 4\left[Cu^I\right]^+ \tag{2}$$
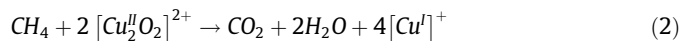
3.2. Modelling of the reaction equilibrium

The adsorption time of the experiments of Fig. 1 was 240 min, which was found to be high enough (as demonstrated latter section 3.3) to ensure the chemisorption reactions reached the equilibrium. The increase of methanol and CO_2 productivities with the methane partial pressure suggests that the chemisorption reactions are reversible. Otherwise, the productivities would be independent of methane partial pressure and dependent only on the
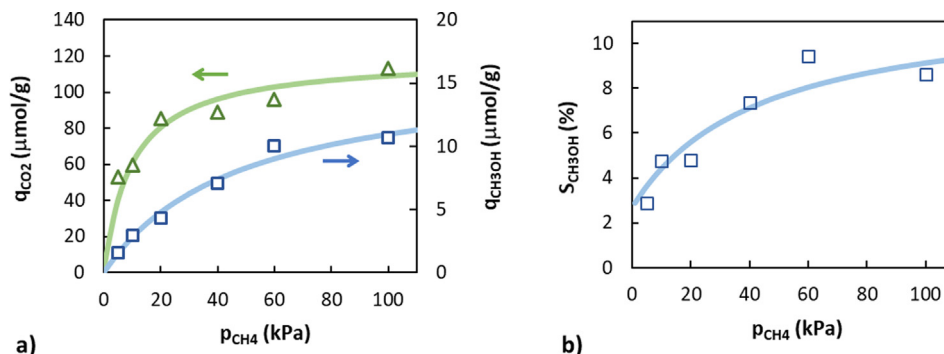
Fig. 1. Influence of methane partial pressure during the adsorption step (adsorption time = 240 min): a) productivity to methanol (□) and CO2 (△), b) selectivity to methanol. Symbols: experiments. Lines: model predictions.

amount of corresponding Cu active species for the reactions. The latter was the same at the beginning of all the tests since the solid was reactivated in the same way. Also, control tests were carried out to ensure that the behaviour is the same in all the successive cycles.

Therefore, the productivities of methanol and CO_2 of Fig. 1a correspond to the chemisorption equilibrium capacities of methoxy (reaction 1) and CO_2 precursor (reaction (2)) species on the copper mordenite, respectively q_{CH_3OH} and q_{CO_2-pr}. The chemisorption equilibrium of these species has been modelled using the Langmuir isotherm, which assumes the molecules can only be adsorbed in a certain number of sites energetically homogeneous and without interaction between adsorbed species (Seabra et al., 2019; Vilarrasa-García et al., 2017). Table 1 summarizes the models for the chemisorption of methoxy (reaction 1) and CO_2 precursors (reaction (2)), where q_{it} are the total solid capacities (μmol g zeolite^{-1}) and K_i are the equilibrium constants (kPa^{-1}).

The model parameters have been fitted by least-square regression using the experiments of Fig. 1a. Model predictions are depicted as solid lines. As can be observed, the models show a good agreement to the experimental data (R^2 = 0.99). The total chemisorption capacities of the solid (q_{it}) are a measurement of total amount of active sites available for the two reactions at the beginning of the chemisorption. In case the reactions were shifted toward products, the productivity would match the chemisorption capacity. The equilibrium constants (K_i) are related to the interaction strength between the chemisorbed species and the solid at 200 °C. The ratio K_2/K_1 is 4.9, which means that the chemisorbed strength of the CO_2 precursors is higher than that of the methoxy species. In this case, methanol equilibrium selectivity can only be raised by increasing methanol partial pressure, so that the reaction equilibrium is shifted for both reactions. This was observed in the experiments of Fig. 1b. The maximum methanol selectivity is 12%, as determined from total chemisorption capacities of the solid.

3.3. Modelling of the reaction kinetics

To measure the rate of the chemisorption process, additional tests have been done using different contacting times with the methane stream. Fig. 2 shows the experimental results for 20
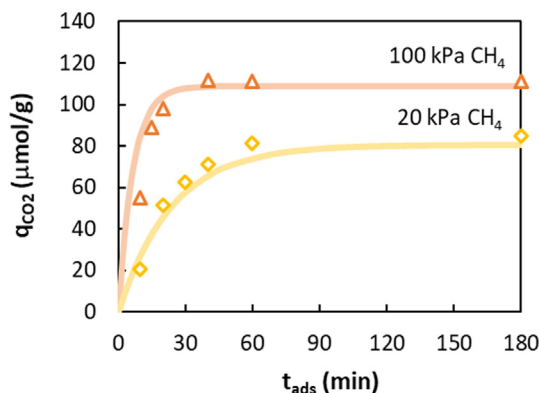
Table 1
Reaction equilibrium models and fitted parameters.

Model	Parameters
$q_{CH_3OH} = \dfrac{q_{1t}K_1 p_{CH_4}}{1+K_1 p_{CH_4}}$	q_{1t} = 16 ± 4 μmol g zeolite^{-1} K_1 = 0.021 ± 0.011 kPa^{-1}
$q_{CO_2-pr} = \dfrac{q_{2t}K_2 p_{CH_4}}{1+K_2 p_{CH_4}}$	q_{2t} = 119 ± 17 μmol g zeolite^{-1} K_2 = 0.103 ± 0.093 kPa^{-1}

Fig. 2. Productivity of CO_2 as a function of the length of the adsorption step. Methane partial pressure: 20 kPa (◇) and 100 kPa (△). Symbols: experiments. Lines: model predictions.

and 100 kPa methane partial pressures. As shown, on increasing the adsorption time, the chemisorption capacity increased. Above ca. 60 min of adsorption time, the capacity was constant, which means the reaction equilibrium was reached. Hence, the adsorption time of 240 min considered in the experiments of Fig. 1 was high enough.

Fig. 3 compares the productivities as a function of methane partial pressure and adsorption time (for the case of 20 and 240 min). These tests have shown that the chemisorption time has an important impact on the productivities. For 20 min, the solid has not reacted completely, particularly for the formation of the methoxy species that seems to be a slower reaction. The use of a chemisorption time of 240 min ensured equilibrium conditions and maximized methanol productivity for each methane gas partial pressure.

The reaction mechanism of methanol formation (reaction 1) on dimeric copper species in Cu-mordenite is made of many steps (Jeong et al., 2021): methane activation, C-H bond cleavage, methoxy generation, methanol desorption, and water adsorption. The last two ones take place in the presence of water during the desorption step of the looping process. The energy profiles of the optimized structures calculated by DFT suggests that the rate-determining-step of the reaction mechanism is methane activation (Jeong et al., 2021). Hence, the reaction rate of methanol formation has been modelled according to a kinetic equation of first order on methane partial pressure and the concentration of vacant dimeric copper species, q_1 (see Table 2). The latter has been determined as the difference between the total chemisorption capacity and methoxy concentration ($q_1 = q_{1t} - q_{CH_3OH}$). As found in section 3.2, this reaction is reversible, which has been accounted for using the equilibrium constant fitted previously (Table 1).
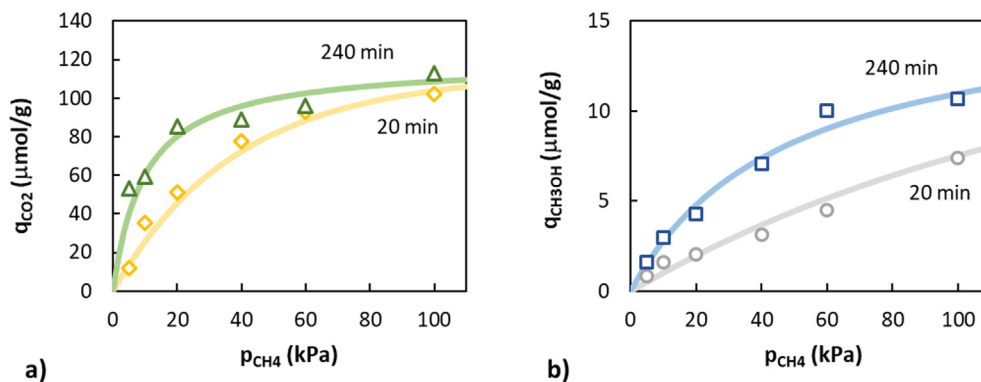
Fig. 3. Influence of methane partial pressure and adsorption time on: a) CO_2 productivity and b) methanol productivity. Symbols: experiments. Lines: model predictions.

Table 2
Reaction kinetic models and fitted parameters.

Model	Parameters
$\frac{dq_{CH_3OH}}{dt} = k_1 \left(p_{CH_4} q_1 - \frac{q_{CH_3OH}}{K_1} \right),$ $q_{CH_3OH}\big|_{t=0} = 0$	$q_1 = q_{1t} - q_{CH_3OH}$ $k_1 = 0.024\ kPa^{-1}h^{-1}$
$\frac{dq_{CO_2-pr}}{dt} = k_2 \left(p_{CH_4} q_2 - \frac{q_{CO_2-pr}}{K_2} \right),$ $q_{CO_2-pr}\big|_{t=0} = 0$	$q_2 = q_{2t} - q_{CO_2-pr}$ $k_2 = 0.085\ kPa^{-1}h^{-1}$

In a similar way, the overoxidation of methane to CO_2 has been described to proceed according to a similar mechanism (Jeong et al., 2021): methane activation, C-H bond cleavage, generation of methoxy, formaldehyde and formate, and carbon dioxide formation and desorption. Considering methane activation also as rate-limiting step, the kinetic equation for the formation of CO_2 precursors of Table 2 is proposed.

The kinetic parameters of the proposed models have been obtained by least-square fitting using the experiments of Figs. 2 and 3. MATLAB lsqcurvefit and ode45 functions have been used to fit and solve the differential equations, respectively. The model predictions have been depicted in the corresponding figures with good agreement to the experimental data.

3.4. Assessment of mass transfer on reaction kinetics

The Cu-mordenite catalyst used in the present work is a microporous material formed by two types of channels: main 12MR (7.0 × 6.5 Å) and perpendicular 8MR pockets (5.7 × 2.6 Å). The size of these channels is slightly larger than the kinetic diameter of the molecules involved in the reaction (methane = 3.8 Å, methanol = 4.3 Å). Therefore, the possibility of mass transfer resistance influencing the chemisorption kinetics has been evaluated.

The effective pore diffusion coefficient at 473 K has been estimated as $2.7 \cdot 10^{-8}\ m^2/s$, based on a Knudsen mechanism and using the textural properties of Cu-mordenite (pore size of 2.6 Å, pore volume of 0.173 cm^3/g and BET surface area of 355 m^2/g). Considering an average solid particle size (0.668 mm) and the adsorption kinetic parameters fitted in section 3.3, the Thiele modulus for intraparticle diffusion was estimated as 0.02 and 0.11, respectively, for the adsorption of methane as methoxy (reaction 1) and CO_2-precursor (reaction (2)) species. The corresponding intraparticle diffusion effectiveness factors were 1 and 0.99, respectively. Consequently, it can be considered that mass transfer limitations were negligible.

3.5. Reaction at aerobic conditions

Many methane feedstocks can be poor and diluted with air, such as, coal bed and ventilation air methane, fugitive emissions of natural gas systems, or biogas generated in landfills and wastewater treatment plants. In these cases, the separation and concentration of methane before upgrading to methanol is advised (Chaemwinyoo et al., 2022; Marín et al., 2020). However, this concentration step can be challenging and costly, so direct upgrading at oxidant conditions can be an alternative. The partial oxidation of methane to methanol on Cu-exchanged zeolites at high oxygen concentrations (ca. 10–16 mol% O_2) was experimentally demonstrated using the looping process in the scope of a previous work (Álvarez et al., 2021). In the light of the previous sections, devoted to the modelling of the reaction at anaerobic conditions, in the present section, the models are extended to the case of aerobic conditions.

The productivity of methanol at aerobic conditions is depicted in Fig. 4. It can be observed that the presence of oxygen produced a decreased in the methanol productivity (Fig. 4a), which is more evident at high methane partial pressures (e.g. 40 kPa), rather than low partial pressures (e.g. 5 and 10 kPa). Thus, high methane partial pressure, and hence high concentration of adsorbed methoxy species, seems to favour methane overoxidation. The tests done for different oxygen partial pressures revealed no dependence on oxygen concentration (Fig. 4b). These findings suggest that the overoxidation may take place by reaction of adsorbed methoxy species and molecular oxygen, as reported in the bibliography (Dinh et al., 2019):

$$Cu^I OCH_3 + H^+ + 3/2\ O_2 \rightarrow CO_2 + 2\ H_2O + \left[Cu^I \right]^+ \tag{3}$$
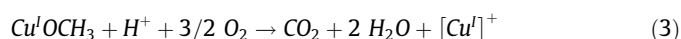
The experiments were carried out at 473 K, which is not enough high to trigger the Cu^+/Cu^{2+} redox cycle and re-activate the catalyst. Temperatures of, at least, 573 K are needed (Sun et al., 2021).

Fig. 5 shows the productivity of the CO_2 precursors (q_{CO_2-pr}) that remained adsorbed on the zeolite at the end of the methane adsorption step. It should be noted that this q_{CO_2-pr} was determined by TPO, right after the adsorption step. Hence, it does not account for the CO_2 generated by over-oxidation with molecular oxygen, and desorbed to the gas phase, during the adsorption step. This CO_2 was experimentally observed by the on-line analysis of the reactor effluent by MS (increase in signal m/z = 44 attributed to CO_2).

The presence of molecular oxygen at high concentration during methane chemisorption leaded to a drastic decrease in the concentration surface CO_2 precursors (Fig. 5). At the end of an anaerobic adsorption step, these species remained adsorbed on the copperzeolite. They were quantified by the TPO carried out after this step. However, at aerobic conditions, the availability of molecular oxygen from the gas phase was able to trigger the complete oxidation of many adsorbed precursors to CO_2, reducing the amount measured by TPO. The experiments of Fig. 5 indicate that the concen-
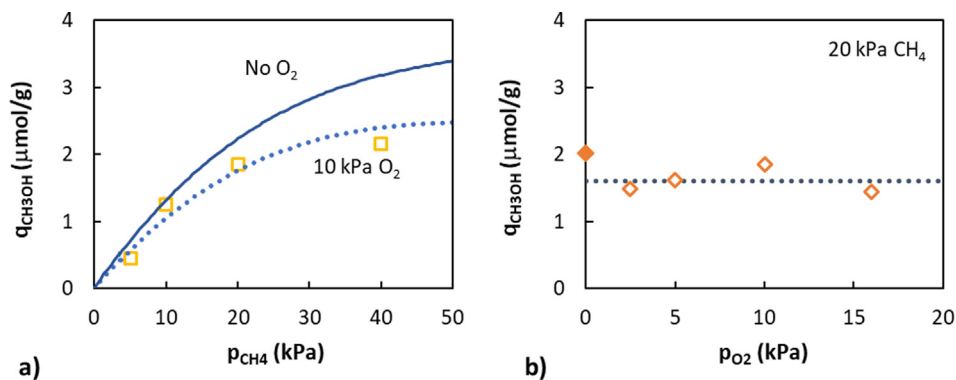
Fig. 4. Influence methane (a) and oxygen (b) partial pressures on methanol productivity at aerobic conditions (adsorption time = 20 min).
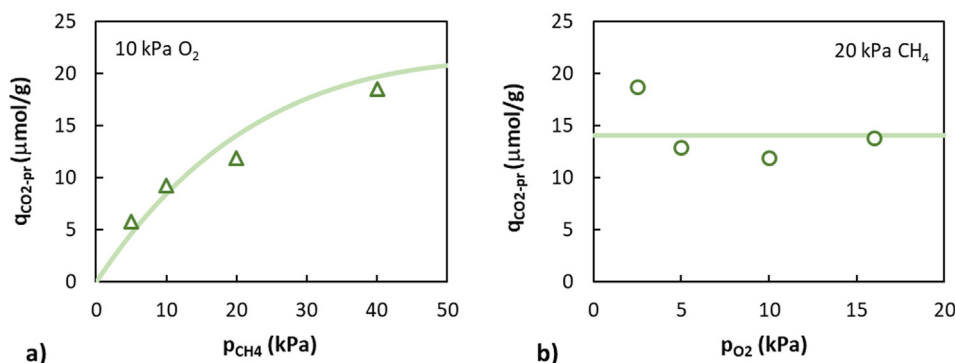

Fig. 5. Influence methane (a) and oxygen (b) partial pressures on the chemisorption of CO_2 precursors at aerobic conditions (adsorption time = 20 min). Symbols: experiments. Line: model prediction.

tration of CO_2 precursors increased, on increasing methane partial pressure, and remained almost unaffected by oxygen partial pressure.

The kinetic model of Table 2 has been completed to account for the over-oxidation to CO_2 of the adsorbed methoxy and CO_2 precursor species, as summarized in Table 3. In agreement with the bibliography (Dinh et al., 2019), these reactions have been considered of first order with respect to the corresponding adsorbed species and order zero with respect to oxygen, as suggested by the experiments of Figs. 4 and 5.

The kinetic constants have been determined by least-square fitting using MATLAB lsqcurvefit and ode45 functions. The model predictions were depicted in Figs. 4 and 5 to assess the quality of the fitting. Overall, the model predicts the trends suggested by the experimental data.

3.6. Application of the process

The studied three-step looping process to convert methane into methanol has shown a low methanol productivity with formation of important amounts of CO_2. For this reason, this process cannot compete with the traditional methanol production process based on methane steam reforming followed by methanol synthesis.

In this work, the looping process has been proposed as an alternative process for the upgrading of methane emissions (with low concentration and possible presence of oxygen), which are not suitable for the methane steam reforming process. The main use of these emissions is typically for thermal purposes and this harnessing can be combined with the production of methanol using the looping process. Thus, the methane emission can be preheated to 200 °C, introduced in a bed loaded with Cu-mordenite, where part of methane is chemisorbed, and the effluent can be sent to a lean turbine to generate electricity from the remaining methane. The methanol product would be recovered from the Cu-mordenite with a steam-desorption step.

4. Conclusions

The partial oxidation of methane to methanol on Cu-mordenite has been studied experimentally in a fixed bed reactor, operated according to a three-step looping process. The methane adsorption step of the process has been studied at anaerobic and aerobic (with high O_2 concentration) conditions.

The experiments revealed that methane chemisorption is a reversible reaction, leading to the formation of methoxy and CO_2-precursors surface species. Adsorption equilibrium models were proposed and fitted for these reactions, using the experiments with a high adsorption time. Conversely, the tests done at different adsorption time were used to fit a kinetic model of first order with respect to methane and the solid active centre.

The process was also studied in the presence of molecular oxygen at high concentration (2.5–16 mol%). This caused a reduction

Table 3
Reaction kinetic models at aerobic conditions and fitted parameters.

Model	Parameters
$\frac{dq_{CH_3OH}}{dt} = k_1\left(p_{CH_4}q_1 - \frac{q_{CH_3OH}}{K_1}\right) - k_3 q_{CH_3OH}$ $q_{CH_3OH}\big|_{t=0} = 0$	$k_3 = 0.0415\ kPa^{-1}h^{-1}$
$\frac{dq_{CO_2-pr}}{dt} = k_2\left(p_{CH_4}q_2 - \frac{q_{CO_2-pr}}{K_2}\right) - k_4 q_{CO_2-pr}$ $q_{CO_2-pr}\big|_{t=0} = 0$	$k_4 = 0.085\ kPa^{-1}h^{-1}$

in methanol productivity, which was particularly noticeable at high methane partial pressures. The presence of molecular oxygen was also responsible of a drastic decrease in the amount of surface CO_2-precursor species, which completed the over-oxidation to CO_2 during the adsorption step. The kinetic models were updated to consider the over-oxidation caused by molecular oxygen.

CRediT authorship contribution statement

Mauro Álvarez: Investigation, Writing – original draft, Investigation, Writing – original draft. **Pablo Marín:** Methodology, Supervision, Validation, Writing – review & editing. **Salvador Ordóñez:** Conceptualization, Supervision, Writing – review & editing, Funding acquisition.

Data availability

Data will be made available on request.

Declaration of Competing Interest

The authors declare that they have no known competing financial interests or personal relationships that could have appeared to influence the work reported in this paper.

Acknowledgement

References

Jackson, R.B., Solomon, E.I., Canadell, J.G., Cargnello, M., Field, C.B., 2019. Methane removal and atmospheric restoration. Nat. Sustain. 2 (6), 436–438.

Pratt, C., Tate, K., 2018. Mitigating Methane: Emerging Technologies To Combat Climate Change's Second Leading Contributor. Environ. Sci. Technol. 52 (11), 6084–6097.

Karakurt, I., Aydin, G., Aydiner, K., 2012. Sources and mitigation of methane emissions by sectors: A critical review. Renew. Energ. 39 (1), 40–48.

Saunois, M., Jackson, R.B., Bousquet, P., Poulter, B., Canadell, J.G., 2016. The growing role of methane in anthropogenic climate change. Environ. Res. Lett. 11 (12), 120207. https://doi.org/10.1088/1748-9326/11/12/120207.

Tomkins, P., Ranocchiari, M., van Bokhoven, J.A., 2017. Direct Conversion of Methane to Methanol under Mild Conditions over Cu-Zeolites and beyond. Acc. Chem. Res. 50 (2), 418–425.

Kulkarni, A.R., Zhao, Z.-J., Siahrostami, S., Nørskov, J.K., Studt, F., 2018. Cation-exchanged zeolites for the selective oxidation of methane to methanol. Catal. Sci. Technol. 8 (1), 114–123.

Latimer, A.A., Kakekhani, A., Kulkarni, A.R., Nørskov, J.K., 2018. Direct Methane to Methanol: The Selectivity-Conversion Limit and Design Strategies. ACS Catal. 8 (8), 6894–6907.

Su, S., Beath, A., Guo, H., Mallett, C., 2005. An assessment of mine methane mitigation and utilisation technologies. Prog. Energy Combust. Sci. 31 (2), 123–170.

Hoglund-Isaksson, L., Winiwarter, W., Purohit, P., Rafaj, P., Schopp, W., Klimont, Z., 2012. EU low carbon roadmap 2050: Potentials and costs for mitigation of non-CO2 greenhouse gas emissions. Energy Strateg. Rev. 1, 97–108.

Fernández, J., Marín, P., Díez, F.V., Ordóñez, S., 2016. Combustion of coal mine ventilation air methane in a regenerative combustor with integrated adsorption: Reactor design and optimization. Appl. Therm. Eng. 102, 167–175.

Marín, P., Díez, F.V., Ordóñez, S., 2019. Reverse flow reactors as sustainable devices for performing exothermic reactions: Applications and engineering aspects. Chem. Eng. Process 135, 175–189.

Marín, P., Vega, A., Díez, F.V., Ordóñez, S., 2020. Control of regenerative catalytic oxidizers used in coal mine ventilation air methane exploitation. Process Saf. Environ. 134, 333–342.

Hammond, C., Conrad, S., Hermans, I., 2012. Oxidative methane upgrading. ChemSusChem 5 (9), 1668–1686.

Sun, L., Wang, Y.u., Guan, N., Li, L., 2020. Methane Activation and Utilization: Current Status and Future. Challenges 8 (8), 1900826. https://doi.org/10.1002/ente.v8.810.1002/ente.201900826.

Zakaria, Z., Kamarudin, S.K., 2016. Direct conversion technologies of methane to methanol: An overview. Renew. Sust. Energ. Rev. 65, 250–261.

Khirsariya, P., Mewada, R.K., 2013. Single Step Oxidation of Methane to Methanol-Towards Better Understanding. Proc. Eng. 51, 409–415.

Han, B., Yang, Y., Xu, Y., Etim, U.J., Qiao, K.e., Xu, B., Yan, Z., 2016. A review of the direct oxidation of methane to methanol, Chinese. J. Catal. 37 (8), 1206–1215.

Olivos-Suarez, A.I., Szécsényi, À., Hensen, E.J.M., Ruiz-Martinez, J., Pidko, E.A., Gascon, J., 2016. Strategies for the Direct Catalytic Valorization of Methane Using Heterogeneous Catalysis: Challenges and Opportunities. Acs Catal. 6 (5), 2965–2981.

Chaemwinyoo, U., Marín, P., Martín, C.F., Díez, F.V., Ordóñez, S., 2022. Assessment of an integrated adsorption-regenerative catalytic oxidation process for the harnessing of lean methane emissions. J. Environ. Chem. Eng. 10 (1), 107013. https://doi.org/10.1016/j.jece:2021.107013.

Palkovits, R., von Malotki, C., Baumgarten, M., Müllen, K., Baltes, C., Antonietti, M., Kuhn, P., Weber, J., Thomas, A., Schüth, F., 2010. Development of Molecular and Solid Catalysts for the Direct Low-Temperature Oxidation of Methane to Methanol. ChemSusChem 3 (2), 277–282.

Mahyuddin, M.H., Shiota, Y., Yoshizawa, K., 2019. Methane selective oxidation to methanol by metal-exchanged zeolites: a review of active sites and their reactivity. Catal. Sci. Technol. 9, 1744–1768.

Liu, Y.F., Du, L., 2018. Theoretical Study of the Oxidation of Methane to Methanol by the [CuIICuII(μ-O)2CuIII(7-N-Etppz)]1+ Complex. Inorg. Chem. 57, 3261–3271.

Jocz, J.N., Medford, A.J., Sievers, C., 2019. Thermodynamic Limitations of the Catalyst Design Space for Methanol Production from Methane. ChemCatChem 11, 593–600.

Al-Shihri, S., Richard, C.J., Al-Megren, H., Chadwick, D., 2020. Insights into the direct selective oxidation of methane to methanol over ZSM-5 zeolites in aqueous hydrogen peroxide. Catal. Today 353, 269–278.

Burnett, L., Rysakova, M., Wang, K., González-Carballo, J., Tooze, R.P., García-García, F.R., 2019. Isothermal cyclic conversion of methane to methanol using copper-exchanged ZSM-5 zeolite materials under mild conditions. Appl. Catal. A-Gen. 587, 117272.

Grundner, S., Markovits, M.A.C., Li, G., Tromp, M., Pidko, E.A., Hensen, E.J.M., Jentys, A., Sanchez-Sanchez, M., Lercher, J.A., 2015. Single-site trinuclear copper oxygen clusters in mordenite for selective conversion of methane to methanol. Nat. Commun. 6, 7546.

Pappas, D.K., Martini, A., Dyballa, M., Kvande, K., Teketel, S., Lomachenko, K.A., Baran, R., Glatzel, P., Arstad, B., Berlier, G., Lamberti, C., Bordiga, S., Olsbye, U., Svelle, S., Beato, P., Borfecchia, E., 2018. The Nuclearity of the Active Site for Methane to Methanol Conversion in Cu-Mordenite: A Quantitative Assessment. J. Am. Chem. Soc. 140 (45), 15270–15278.

Mahyuddin, M.H., Tanaka, T., Staykov, A., Shiota, Y., Yoshizawa, K., 2018. Dioxygen Activation on Cu-MOR Zeolite: Theoretical Insights into the Formation of Cu2O and Cu3O3 Active Species. Inorg. Chem. 57, 10146–10152.

Jeong, Y.R., Jung, H., Kang, J., Han, J.W., Park, E.D., 2021. Continuous Synthesis of Methanol from Methane and Steam over Copper-Mordenite. ACS Catal. 11, 1065–1070.

Knorpp, A.J., Newton, M.A., Pinar, A.B., van Bokhoven, J.A., 2018. Conversion of Methane to Methanol on Copper Mordenite: Redox Mechanism of Isothermal and High-Temperature-Activation Procedures. Ind. Eng. Chem. Res. 57, 12036–12039.

Mahyuddin, M.H., Tanaka, T., Shiota, Y., Staykov, A., Yoshizawa, K., 2018. Methane Partial Oxidation over [Cu2(μ-O)]2+ and [Cu3(μ-O)3]2+ Active Species in Large-Pore Zeolites. ACS Catal. 8 (2), 1500–1509.

Zheng, J., Lee, I., Khramenkova, E., Wang, M., Peng, B.o., Gutiérrez, O.Y., Fulton, J.L., Camaioni, D.M., Khare, R., Jentys, A., Haller, G.L., Pidko, E.A., Sanchez-Sanchez, M., Lercher, J.A., 2020. Importance of Methane Chemical Potential for Its Conversion to Methanol on Cu-Exchanged Mordenite. Chem.-Eur. J. 26 (34), 7563–7567.

Sheppard, T., Daly, H., Goguet, A., Thompson, J.M., 2016. Improved Efficiency for Partial Oxidation of Methane by Controlled Copper Deposition on Surface-Modified ZSM-5. ChemCatChem 8 (3), 562–570.

Sushkevich, V.L., Verel, R., Bokhoven, J.A., 2020. Pathways of Methane Transformation over Copper-Exchanged Mordenite as Revealed by In Situ NMR and IR Spectroscopy. Angew. Chem. 132 (2), 920–928.

Sheppard, T., Hamill, C.D., Goguet, A., Rooney, D.W., Thompson, J.M., 2014. A low temperature, isothermal gas-phase system for conversion of methane to methanol over Cu–ZSM-5. ChemComm 50 (75), 11053–11055.

Knorpp, A.J., Newton, M.A., Pinar, A.B., van Bokhoven, J.A., 2018. Conversion of Methane to Methanol on Copper Mordenite: Redox Mechanism of Isothermal and High-Temperature-Activation Procedures. Ind. Eng. Chem. Res. 57 (36), 12036–12039.

Sun, L., Wang, Y.u., Wang, C., Xie, Z., Guan, N., Li, L., 2021. Water-involved methane-selective catalytic oxidation by dioxygen over copper zeolites. Chem 7 (6), 1557–1568.

Álvarez, M., Marín, P., Ordóñez, S., 2020. Direct oxidation of methane to methanol over Cu-zeolites at mild conditions. Mol. Catal. 487, 110886. https://doi.org/10.1016/j.mcat.2020.110886.

Álvarez, M., Marín, P., Ordóñez, S., 2021. Harnessing of Diluted Methane Emissions by Direct Partial Oxidation of Methane to Methanol over Cu/Mordenite. Ind. Eng. Chem. Res. 60 (26), 9409–9417.

Grundner, S., Luo, W., Sanchez-Sanchez, M., Lercher, J.A., 2016. Synthesis of single-site copper catalysts for methane partial oxidation. ChemComm 52 (12), 2553–2556.

Alayon, E.M., Nachtegaal, M., Ranocchiari, M., van Bokhoven, J.A., 2012. Catalytic conversion of methane to methanol over Cu–mordenite. ChemComm 48 (3), 404–406.

Brezicki, G., Zheng, J., Paolucci, C., Schlögl, R., Davis, R.J., 2021. Effect of the Co-cation on Cu Speciation in Cu-Exchanged Mordenite and ZSM-5 Catalysts for the Oxidation of Methane to Methanol. ACS Catal. 11 (9), 4973–4987.

Sushkevich, V.L., van Bokhoven, J.A., 2018. Effect of Brønsted acid sites on the direct conversion of methane into methanol over copper-exchanged mordenite. Cataly. Sci. Technol. 8 (16), 4141–4150.

Sushkevich, V.L., Verel, R., Bokhoven, J.A., 2020. Pathways of Methane Transformation over Copper-Exchanged Mordenite as Revealed by In Situ NMR and IR. Spectroscopy 59 (2), 910–918.

Seabra, R., Ribeiro, A.M., Gleichmann, K., Ferreira, A.F.P., Rodrigues, A.E., 2019. Adsorption equilibrium and kinetics of carbon dioxide, methane and nitrogen on binderless zeolite 4A adsorbents. Micropor. Mesopor. Mater. 277, 105–114.

Vilarrasa-García, E., Cecilia, J.A., Azevedo, D.C.S., Cavalcante, C.L., Rodríguez-Castellón, E., 2017. Evaluation of porous clay heterostructures modified with amine species as adsorbent for the CO2 capture. Micropor. Mesopor. Mat. 249, 25–33.

Marín, P., Yang, Z., Xia, Y., Ordóñez, S., 2020. Concentration of unconventional methane resources using microporous membranes: Process assessment and scale-up. J. Nat. Gas Sci. Eng. 81, 103420.

Dinh, K.T., Sullivan, M.M., Narsimhan, K., Serna, P., Meyer, R.J., Dincă, M., Román-Leshkov, Y., 2019. Continuous Partial Oxidation of Methane to Methanol Catalyzed by Diffusion-Paired Copper Dimers in Copper-Exchanged Zeolites. J. Am. Chem. Soc. 141, 11641–11650.